Journal of Autoimmunity 121 (2021) 102660

Contents lists available at ScienceDirect

Journal of Autoimmunity

journal homepage: www.elsevier.com/locate/jautimm

Mesenchymal stromal cells-derived extracellular vesicles alleviate systemic sclerosis via miR-29a-3p

Pauline Rozier [a], Marie Maumus [a], Alexandre Thibault Jacques Maria [a,b], Karine Toupet [a], Joséphine Lai-Kee-Him [c], Christian Jorgensen [a,d], Philippe Guilpain [a,b], Danièle Noël [a,d,*]

[a] IRMB, University of Montpellier, INSERM, Montpellier, France
[b] Department of Internal Medicine, Multi-organic Diseases, CHU, Montpellier, France
[c] Centre de Biochimie Structurale (CBS), University of Montpellier, INSERM, CNRS, Montpellier, France
[d] Clinical Immunology and Osteoarticular Disease Therapeutic Unit, Department of Rheumatology, CHU, Montpellier, France

ARTICLE INFO

Keywords:
Exosomes
Extracellular vesicles
Scleroderma
Mesenchymal stem cells
miR-29a
DNMT3A
PDGFRBB

ABSTRACT

Systemic sclerosis (SSc) is a potentially lethal disease with no curative treatment. Mesenchymal stromal cells (MSCs) have proved efficacy in SSc but no data is available on MSC-derived extracellular vesicles (EVs) in this multi-organ fibrosis disease. Small size (ssEVs) and large size EVs (lsEVs) were isolated from murine MSCs or human adipose tissue-derived MSCs (ASCs). Control antagomiR (Ct) or antagomiR-29a-3p (A29a) were transfected in MSCs and ASCs before EV production. EVs were injected in the HOCl-induced SSc model at day 21 and euthanasized at day 42. We found that both ssEVs and lsEVs were effective to slow-down the course of the disease. All disease parameters improved in skin and lungs. Interestingly, down-regulating miR-29a-3p in MSCs totally abolished therapeutic efficacy. Besides, we demonstrated a similar efficacy of human ASC-EVs and importantly, EVs from A29a-transfected ASCs failed to improve skin fibrosis. We identified Dnmt3a, Pdgfrbb, Bcl2, Bcl-xl as target genes of miR-29a-3p whose regulation was associated with skin fibrosis improvement. Our study highlights the therapeutic role of miR-29a-3p in SSc and the importance of regulating methylation and apoptosis.

1. Introduction

Systemic sclerosis (SSc) is a rare, life-threatening autoimmune disease for which no curative treatment is available to date [1]. Current treatments are essentially palliative and associate symptomatic support with organ transplantation or immunosuppressive drug therapy, which may cause severe side effects [2]. Hematopoietic stem cell transplantation has proved to be a major step forward, but here again, at the expense of heavy side effects [3]. Promising therapeutic options include mesenchymal stromal/stem cell (MSC)-based therapy, which has shown efficacy in several animal models of SSc. The therapeutic interest of bone marrow- and adipose tissue-derived MSCs has already been demonstrated in murine models [4,5]. Moreover, clinical studies report encouraging results (for review, see Ref. [5]).

The therapeutic effect of MSCs is mediated primarily through the secretion of soluble factors that can be conveyed within extracellular vesicles (EVs). EVs are classified into three major subtypes depending on their size and biogenesis. Apoptotic bodies are the largest vesicles (500–1500 nm) released by apoptotic cells, microvesicles/microparticles are large vesicles (120–500 nm) budding from the plasma membrane and exosomes are small vesicles (50–150 nm) originating from the endosomal compartment [6]. However, because of overlapping sizes between subtypes, current isolation procedures generally lead to the isolation of small size vesicles (ssEVs) or large size vesicles (lsEVs) that cannot discriminate the vesicles by their origin [7]. EVs are carriers of a variety of bioactive factors including proteins, lipids, DNA, mRNA and miRNAs that play important functions in intercellular communication. Recently, the therapeutic function of MSC-derived EVs (MSC-EVs) has gained much attention in various diseases, including autoimmune and rheumatic diseases [8], and in various animal models of diseases (for review, see Ref. [9]). However, to our knowledge, no data is available on the therapeutic function of MSC-EVs for skin fibrosis and more importantly, in a multi-organ fibrotic disorder such as SSc.

Among the mediators conveyed within MSC-EVs, miRNAs are reported to take a large part in their therapeutic effect. Numerous miRNAs could have functional relevance for fibrotic diseases by modulating the

* Corresponding author. Inserm U1183, IRMB, Hôpital Saint-Eloi, 80 avenue Augustin Fliche, 34295, Montpellier cedex 5, France.
E-mail address: daniele.noel@inserm.fr (D. Noël).

https://doi.org/10.1016/j.jaut.2021.102660
Received 16 April 2021; Received in revised form 7 May 2021; Accepted 9 May 2021
Available online 19 May 2021

profile of mRNAs and consequently, proteins in target cells (for review, see Ref. [9]). One of these miRNAs, miR-29a gained interest in the context of scleroderma. Indeed, miR-29a was shown to be decreased in hair, serum and dermal fibroblasts from scleroderma patients [10–12]. It was strongly down-regulated in fibroblasts and skin sections from SSc patients as well as in the bleomycin model of skin fibrosis and an inverse correlation between miR-29a and type I collagen was demonstrated [13]. In addition to type I collagen, miR-29a was found to target TGFβ activated kinase 1 binding protein 1 (TAB1), thereby reducing TIMP1 expression and increasing matrix metalloproteinase 1 (MMP1) [14,15]. Moreover, miR-29a has been described as a potent inducer of apoptosis in SSc fibroblasts by disrupting the production of anti-apoptotic factors (Bcl-2, Bcl-XL) [16]. Therefore, miR-29a has been described as an anti-fibrotic and pro-apoptotic factor with potential therapeutic interest in SSc.

In the present study, we investigated the capacity of MSC-EVs to improve skin and lung fibrosis in a multi-organ fibrotic disorder, using the relevant HOCl-induced murine model of SSc. We determined the respective role of ssEVs and lsEVs from murine MSCs and that of EVs from human adipose tissue derived MSCs (ASC-EVs) in attenuating SSc clinical course. We focused our study on miR-29a as a potential anti-fibrotic factor conveyed within EVs, and its downstream targets to decipher its mechanism of action in SSc. Importantly, we provide evidence that miR-29a-3p targets apoptosis and methylation-related genes.

2. Methods

2.1. Murine and human cell culture

Murine MSCs were isolated from the bone marrow of C57BL/6 mice and expanded in proliferative medium (DMEM, 10% fetal calf serum (FCS), 2 mmol/mL glutamine, 100 μg/mL penicillin/streptomycin). They were characterized by phenotyping and tri-lineage differentiation potential, as reported [17] and used at passage 12–18. Human healthy ASCs were isolated from adipose tissue. All individuals gave written consent and approval was obtained from the French Ministry of Higher Education and Research (DC-2009-1052). ASCs were cultured in αMEM medium containing 10% FCS, 100 μg/mL penicillin/streptomycin, 2 mmol/mL glutamine and 1 ng/mL basic fibroblast growth factor (bFGF) (R&D Systems), characterized as in Ref. [18] and used at passage 1–3.

2.2. Cell transfection

MSCs and ASCs were transfected with 50 nM of antagomiR-control (ACt) or antagomiR-29a-3p (A29a) overnight (ON), using Oligofectamine (ThermoFisher Scientific). Supernatants were collected 48 h after transfection.

2.3. Production and isolation of EVs

MSCs and ASCs were seeded at 7×10^4 cells/cm^2 and cultured for 24 h. The medium was then replaced by the production medium consisting of DMEM or αMEM, for MSCs and ASCs respectively, containing 100 μg/mL penicillin/streptomycin, 2 mmol/mL glutamine and 3% EV-free FCS. This latter was obtained after ultracentrifugation of medium containing 20% FCS at 100,000 g, ON. After 48 h for MSCs or 60 h for ASCs, conditioned supernatants were centrifuged at 300 g, 4 °C for 10 min to eliminate cells and 2500 g, 4 °C for 25 min to remove debris and apoptotic bodies. Subsequently, media were centrifuged at 18,000 g, 4 °C for 1 h to pellet lsEVs and, then at 100,000 g for 2 h to pellet ssEVs. Pellets obtained at each step were submitted to a second round of centrifugation at 100,000 g, 4 °C for 2 h and suspended in 100 μL of phosphate buffer saline (PBS). More than 95% viability and less than 15% apoptosis of producing cells, assessed by Annexin V/7AAD labelling and flow cytometry, were required before EV recovery. EV preparations were kept at 4 °C ON and used as freshly prepared EV suspensions, except for the experiment with frozen EVs, which were kept at −80 °C before use.

2.4. EV characterization

EVs were characterized as recommended by the International Society of Extracellular Vesicles (ISEV) [7]. Total protein content of EV suspensions was quantified using the Micro BCA Protein Assay Kit (ThermoFisher Scientific). Number and size of particles were determined by nanotracking analysis (NanoSight NS300, Orsay). EV phenotype was determined by flow cytometry after EV incubation with 2 μL of aldehyde/sulfate latex beads (4 μm, 4% W/V, ThermoFisher Scientific) at 4 °C ON and glycine (100 mM) addition for 30 min. EV-coated beads were labelled with fluorophore-conjugated antibodies for murine CD9, CD11b, CD29, CD44, CD45, CD63, CD81, Sca-1 (BD Biosciences) for 30 min. For cryoTEM analysis, EVs were applied to glow discharged Lacey grid (Ted Pella inc.), blotted for 1s and then flash frozen in liquid ethane using a CP3 cryo-plunge (Gatan inc.). Cryo-EM was carried out on a JEOL 2200FS FEG operating at 200 kV under low-dose conditions in the zero-energy-loss mode with a slit width of 20 eV.

2.5. Western blot

Samples were lysed in 50 μL of RIPA containing 1/100 protease inhibitor (Sigma). Ten μg of proteins were loaded on 4–12% SDS polyacrylamide gel (Life Technologies) and run at 200 V for 30 min. Protein transfer to nitrocellulose membrane was performed for 7 min using iBlot™2 Dry blotting system (ThermoFisher Scientific). Membranes were blocked with 5% skim milk in TBS and incubated ON at 4 °C with primary antibodies: anti-Tsg101 (1/200), anti-Alix (1/100), anti-ApoA1 (1/200) from Santa Cruz and at room temperature for 2 h with anti-Actin (1/5000; Sigma). Blots were revealed using WesternBright Sirius HRP substrate (Advansta) and quantified with ChemiDoc MP imager and Image Lab Software (Bio-Rad).

2.6. Animal experimentation

HOCl-induced SSc murine model was approved by the Regional Ethics Committee on Animal Experimentation (APAFIS#5351201605091907918 7). Six-week-old female BALB/cJRj mice (Janvier Labs) were cared for according to the European guidelines for the care and use of laboratory animals (2010/63/UE). Surgery and euthanasia were performed after anaesthesia with isoflurane gas, and all efforts were made to minimize suffering. Mice were housed in solid bottomed plastic cages in quiet rooms at 22° ± 1 °C, 60% controlled humidity, and 12 h/12 h light/dark cycle. Animals were used after an adaptation period of 7 days and had free access to tap water and standard pelleted chow. Backs of mice were shaved the day before disease induction. Skin thickness was measured with a caliper and once a week thereafter. HOCl solutions were prepared extemporaneously by adding NaClO (9.6%) to KH2PO4 solution (100 mM, pH 6.2) to get the desired HOCl concentration, defined by optical density of 0.7–0.9 at 292 nm (Nanodrop, Thermoscientific). Daily prepared HOCl (150 μL) was injected into two sites in the back of mice, 5 days a week for 6 weeks. Treatment groups were done at day 21 to homogenize the mean skin thickness in each group of 7–8 mice before PBS (control group), cell or EV intravenous injections (100 μL). Animal number in each group was calculated using G Power software and data from previous experiments; no criteria for exclusion/inclusion was set and none was excluded. Treatment groups were mixed in cages to allow blinding and minimize bias. At day 42, mice were sacrificed and blood, skin biopsies (6 mm punchs) and lungs were recovered. Samples were stored at −80 °C for RT-qPCR or fixed in 4% formaldehyde for histology.

2.7. Histopathological and immunohistopathological analyses

Skin and lung samples were processed for routine histology. Masson trichrome staining or immunostaining were performed using antibodies specific for αSma (1/100; Abcam), TGFβ (1/200; Abcam) or DAPI (1/1000; Sigma). Histological slides were scanned with Nanozoomer (Hamamatsu) and dermal thickness was measured with NDP.view2 software. Images of slides were acquired on a confocal laser scanning microscope (TCS SP5-II, Leica Microsystems). Image stacks were analyzed with Image J software.

2.8. RNA extraction and RT-qPCR

Total RNA was extracted from skin and lung samples after mechanical dissociation and using the RNeasy Mini Kit (Qiagen, Courtaboeuf). Reverse transcription was performed on 0.5 μg RNA using 100 U of M-MLV reverse transcriptase (ThermoFisher Scientific). Real time PCR was performed on 20 ng cDNA using specific primers (Supl. Table) and SYBR Green I Master mix (Roche Diagnostics). Values were normalized to TATA binding protein (*Tbp*) housekeeping gene and expressed as relative expression or fold change using the respective formulae $2^{-\Delta CT}$ or $2^{-\Delta\Delta Ct}$.

MiRNA extraction was performed using the miRNeasy Micro Kit (Qiagen). Reverse transcription was performed on 150 ng RNA using TaqMan® MicroRNA Reverse Transcription Kit (ThermoFisher Scientific). Real time PCR was performed on 10 ng cDNA using Taqman microRNA hsa-miR29a-3p (Life Technologies) and Taqman Master Mix II no UNG (Life Technologies). Values were normalized to Ct for MSCs, ASCs and EVs.

2.9. Statistical analysis

Statistical analyses were performed using GraphPad 8 Prism Software. Data were analyzed by comparing a single group with the control group using the Student *t*-test for values with a normal distribution or the Mann-Whitney test when values did not show normal distribution, as evaluated using the Shapiro-Wilk normality test. For normalized values, a one sample *t*-test or Wilcoxon test were performed when values were parametric or non-parametric, respectively. Data are presented as mean ± SEM.

3. Results

3.1. Both MSC-EV subtypes stop disease progression in murine HOCl-induced SSc

Before investigating the therapeutic effect of MSC-EVs in SSc, we first characterized the two EV subtypes recovered by differential ultracentrifugation. SsEVs with a mean size of 158 nm were isolated at 100,000 g while a more heterogenous population of lsEVs with a mean size of 191 nm was isolated at 18,000 g (Fig. 1A). The median size of ssEVs (145 nm) was significantly lower than that of lsEVs (165 nm). The number of particles produced by MSCs was significantly higher for ssEVs than lsEVs (1.5–2 fold more) when reported to 10^6 cells or 1 μg of total proteins (Fig. 1A). The two subtypes were characterized by a bilayer membrane as visualized by cryoTEM (Fig. 1B). They were negative for hematopoietic markers (CD11b, CD45), positive for MSC markers (CD29, Sca-1, CD44) and markers of the endosomal compartment (CD9, CD63, CD81). All endosomal markers were expressed at higher levels on ssEVs (Fig. 1C). Western blot analysis revealed absence of ApoA1, indicative of low contamination by serum proteins while expression of Alix and Tsg101 was detected with ssEVs and only Alix with lsEVs (Fig. 1D and E). These data support that ssEV and lsEV populations released by MSCs exhibit slightly different characteristics.

We then compared the course of HOCl-induced SSc between a group of control mice and three groups that were treated with 2.5×10^5 MSCs or 250 ng of ssEVs or lsEVs (the approximate quantity of particles produced by 2.5×10^5 MSCs for 48 h). Skin thickness increase was stopped and thickness was significantly lower in all treated groups than in control group at sacrifice (Fig. 2A). Clinical data were confirmed by histology as shown by representative skin sections and dermal thickness measures that were significantly lower in all treated groups (Fig. 2B and C). Mice treated with ssEVs exhibited less severe involvement with lower dermal thickness than other treated groups. Immunohistological analysis revealed lower cellularity and lower expression of *Tgfβ1* and *αSma* (Fig. 2C). At the molecular level, expression of several fibrotic (*Col1a1, Tgfβ1, TgfβR2, αSma*) or inflammatory (*IL1β*, *Tnfα*) markers was significantly decreased and markers of remodeling (*Mmp9, Mmp1, Timp1*) were improved (Fig. 2D). In the lungs, cellular infiltrates were smaller and low amounts of fibrotic tissue were observed in the pulmonary parenchyma, regardless of treatment (Fig. 2E). The molecular analysis confirmed improvement with lower expression of fibrotic, inflammatory and remodeling markers (Fig. 2F). Altogether, the data indicated that both types of EVs attenuated disease symptoms.

3.2. miR-29a-3p is responsible for the therapeutic effect of MSCs in SSc

The next step was to investigate the role of miR-29a in the therapeutic effect of MSCs. The more predominant mature form of miR-29a is miR-29a-3p [19]. We therefore transfected MSCs with premiR-29a-3p and showed that transfected MSCs expressed 300-fold more miR-29a-3p than control MSCs. However, the therapeutic effect of miR-29a-3p-over-expressing MSCs was similar to control MSCs in the model of HOCl-induced SSc (data not shown). We then down-regulated miR-29a-3p in MSCs using antagomiR-29a-3p (MSC-A29a). Expression of miR-29a-3p was down-deregulated by 80% as compared to MSCs transfected with control antagomiR (MSC-ACt) at day 0 (Fig. 3A). Interestingly, injection of MSC-A29a did not stop disease progression, by contrast to MSC-ACt or non-transfected MSC (MSC-NT) (Fig. 3B). Consistently, skin thickness at sacrifice was lower in the MSC-NT and MSC-ACt groups than in control HOCl group but similar in the MSC-A29a and control groups. Similar observations were obtained by histological analysis of skin sections and measures of dermal thickness (Fig. 3C and D). At the molecular level, expression of fibrotic, remodeling and inflammatory markers was not improved in MSC-A29a group compared to HOCl control group, except for *Col3a1* and the *TgfβRII/Tgfβ1* and *Mmp1/Timp1* ratios (Fig. 3E). Moreover, all markers were significantly worsened in MSC-A29a group compared to MSC-ACt group. High expression of *Tgfβ1* and *αSma* proteins was detected in skin sections from MSC-A29a and control groups while low expression was detected in MSC-ACt and MSC-NT groups (Fig. 3F). Altogether, our results demonstrated that miR-29a-3p mediates the therapeutic effect of MSCs in SSc skins.

3.3. Human ASC-EVs improve SSc clinical signs and convey miR-29a-3p

We thereafter investigated the possibility that miR-29a-3p could be delivered by EVs that are released by MSCs. We indeed detected miR-29a-3p in both ssEVs and lsEVs isolated from MSCs (Fig. 4A, left panel). To explore the role of miR-29a-3p in MSC-EVs, we used a loss-of-function approach and down-regulated the expression of miR-29a-3p in MSCs by antagomiR-29a-3p transfection before EV recovery from two days-conditioned supernatants. Unfortunately, similar levels of miR-29a-3p were quantified in MSC-A29a and MSC-ACt (data not shown). This was attributed to the dilution of A29a in proliferating MSCs. We therefore decided to use human ASCs, which express miR-29a-3p at similar levels as murine MSCs (Fig. 4A, middle and left panels) and proliferate at lower rate. After transfection of antagomiR-29a-3p, expression of miR-29a-3p was inhibited in ASCs (ASC-A29a) by 80% at day 0 and by 50% at day 2 (Fig. 4A, right panel). These data indicated that miR-29a-3p expression can be down-regulated in ASCs for at least 2 days allowing EV production. Total EVs were then isolated from ASCs

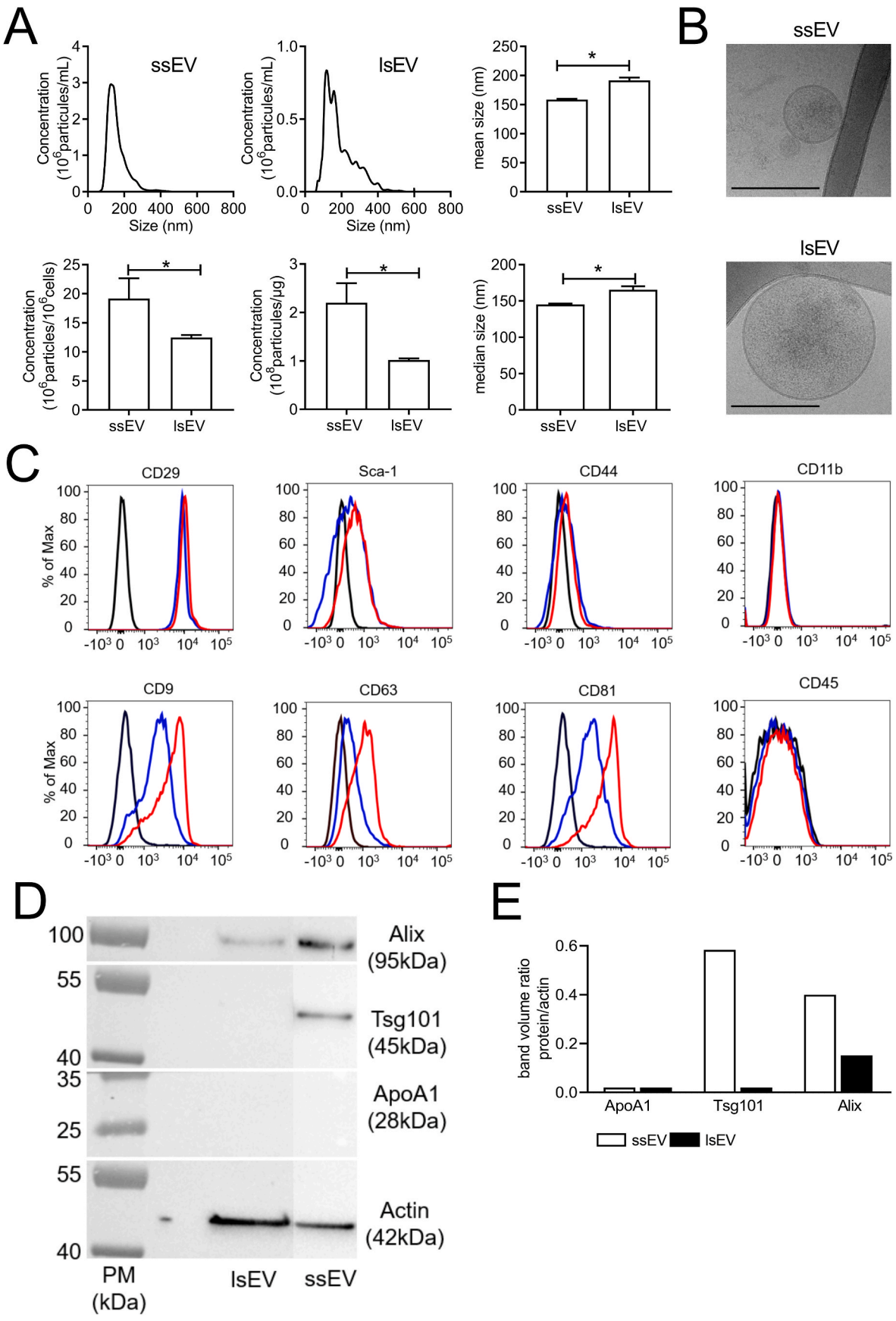

(caption on next page)

Fig. 1. Characterization of extracellular vesicles isolated from murine mesenchymal stromal cells. (A) Size distribution of small size and large size extracellular vesicles (ssEVs and lsEVs) assessed by NanoTracking Analysis. EV concentration is expressed as particle numbers produced by 10^6 cells or per μg of total proteins. Mean and median sizes of EVs are indicated (n = 3). (B) Cryo-transmission electron microscopy images of ssEVs and lsEVs (scale bar, 200 μm). (C) Immunophenotyping of ssEVs (red), lsEVs (blue) and isotype control (black). Expression of markers from parental cells (CD29, Sca-1, CD44), hematopoietic cells (CD11b) and exosomes (CD9, CD63, CD81) is analyzed by flow cytometry. (D) Western blot analysis of endosomal (Alix, Tsg101) and serum (ApoA1) markers in ssEV and lsEV protein extracts. (E) Quantification of proteins shown in (D). *: $p < 0.05$. (For interpretation of the references to colour in this figure legend, the reader is referred to the Web version of this article.)

using the same conditions as those used for MSC-EVs but suppressing the 18,000 g step. Total EVs were chosen because no differential effect of ssEVs and lsEVs from murine MSCs was previously demonstrated. ASC-EVs displayed a heterogeneous size profile with a median and modal size of 129.2 ± 0.88 nm and 106.9 ± 10.9 nm, respectively (Fig. 4B). Production of ASC-EVs was estimated at 307 ± 15 particles/ASC and 1.74 particles/μg total proteins. Particles with a bilayer membrane were observed by CryoTEM (Fig. 4C). ASC-EVs expressed markers of endosomal compartment (CD9, CD63, CD81) and parental cells (CD29, CD44, CD73, CD90) and did not express CD45 or CD11b confirming the phenotype of ASC-EVs (data not shown). Importantly, presence of miR-29a-3p was detected in ASC-EVs (Fig. 4A, middle panel).

We then evaluated the efficacy of ASC-EVs in the SSc model. ASC-EVs (4×10^7 particles) were injected either as freshly isolated suspension (EV-fresh) or as thawed suspension after preservation at −80 °C (EV-frozen). This amount of particles was the quantity produced by 2.5×10^5 ASCs during 48 h. Both EV-fresh and EV-frozen efficiently stopped disease progression and reduced skin thickness as measured at sacrifice (Fig. 4D). They also reduced fibrosis as shown on histological sections and improved markers of fibrosis, remodeling and inflammation (Fig. 4E and F). The data indicated that EVs from human ASCs were efficient to attenuate clinical symptoms and reduce fibrotic, remodeling and inflammatory markers in murine SSc. Short-term preservation of ASC-EVs at −80 °C did not alter their functional properties.

3.4. *MiR-29a-3p delivered by ASC-EVs contributes to their therapeutic effect*

EVs were then recovered from ASCs transfected with antagomiR-29a-3p (EV-A29a). They contained lower levels of miR-29a-3p (78% less) than EVs from antagomiR-control ASCs (EV-ACt) (Fig. 5A). In SSc, EV-A29a did not reverse the disease course and did not prevent the skin thickness increase as measured at day 42 (Fig. 5B and C). Higher collagen deposition and fibrotic lesions were observed on skin histological samples in the EV-A29a group compared to EV-ACt (Fig. 5D). In accordance, expression levels of *Tgfβ1, αSma, Mmp9, IL1β* did not improve and expression of all markers was higher in EV-A29a group compared to EV-ACt group, even though not all reached statistical significance (Fig. 5E). In lungs, expression of *αSma* and *Tgfβ1* was significantly higher in EV-A29a treated mice (Fig. 5F).

Finally, we focused on the potential mechanism of action of miR-29a-3p in SSc fibrotic tissues and investigated the expression of already validated targets. We confirmed an increased expression of *Col1a1, Col3a1* and of *Mmp9, Timp1* in the skin of SSc mice treated with MSC-A29a and EV-29a (Fig. 3E; 5E). We also detected that anti-apoptotic markers *Bcl2* and *Bcl-xl* were significantly up-regulated while the pro-apoptotic marker *Bax* was not significantly modulated (Fig. 6A). In addition, we found out that the DNA demethylase Ten-Eleven translocation methylcytosinedioxygenase 1 (*Tet1*), the DNA methyltransferase 3A (*Dnmt3a*) and platelet-derived growth factor receptor B (*Pdgfrbb*) were significantly down-regulated in MSC-NT, MSC-Act and EV-ACT-treated mice (Fig. 6B). By contrast, these factors were expressed at higher levels in skin from MSC-A29a and EV-29a treated mice compared to MSC-ACt or EV-ACT-treated mice. These data argued that miR-29a-3p mediates in a large part the therapeutic effect of ASC-EVs in the murine model of SSc by modulating the expression of multiple markers that are deregulated in SSc.

4. Discussion

This study reports the first demonstration that EVs isolated from murine MSCs and human ASCs exert a therapeutic effect in a relevant systemic model of scleroderma, by halting the clinical symptoms, limiting collagen fiber accumulation in skin and lungs as well as improving the molecular markers of fibrosis, remodeling and inflammation. We also provide evidence that miR-29a-3p is one key mediator, responsible for EV-mediated improvement of SSc by targeting several genes deregulated during the course of the disease.

Previous studies have reported that either total EVs or ssEVs, frequently called exosomes, can reduce fibrosis in different organs (for review, see Ref. [9]). Nevertheless, few studies have investigated the therapeutic role of EVs in SSc, most of them focusing on EVs as diagnosis and follow-up tools (for review, see Ref. [20]). They reported an increased secretion of exosomes by SSc dermal fibroblasts and a higher number of particles in the serum of SSc patients, even though patients with cutaneous ulcers exhibited a significantly reduced number of vesicles [21]. A possible role of EVs in the pathogenesis of the disease was therefore suggested. After internalization by target cells, EVs might induce a pro-fibrotic molecular program and be involved in the disease propagation/maintenance [22]. However, only one study has reported the therapeutic interest of EVs in SSc. Indeed, exosomes isolated from bone marrow-derived MSCs were shown to rescue the osteopenic phenotype of tight-skin (*Tsk/*$^+$) mutant mice, a genetic murine model of SSc, characterized by osteopenia and skin fibrosis, through the transfer of miR-151-5p [23]. Our data are in line with their findings although the authors did not test the direct effect of exosomes on skin and lung fibrosis but reported the beneficial role of adenovirally expressed miR-151-5p on these organs. Here, we showed that both ssEV and lsEV subtypes were equally efficient to protect mice from skin and lung fibrosis through the modulation of fibrotic, remodeling and inflammatory genes.

We also found that total EVs from human ASCs exert similar therapeutic effect as murine EV subtypes. Similar findings were previously reported comparing murine BM-MSCs and human ASCs or BM-MSCs in the HOCl-induced murine model of SSc [4]. This suggests similar mechanisms of action exerted by MSCs from the two species and mainly through the release of EVs. Of note, both freshly prepared and frozen EVs were efficient to stop the course of the disease. This result was of interest for manufacturing and clinical application of EVs because we previously showed that cryopreservation of MSC-EVs may impact their immunosuppressive properties [24]. We found that the median size of frozen EVs was lower compared to fresh EVs suggesting a loss of the largest size EVs and/or destabilization and reorganization of EV structure [24]. Formation of multilamellar EV structures was clearly identified by cryoTEM analysis (data not shown) and impact of storage-induced changes on bioactivity still remains unclear [25]. Upon freezing-thawing of EV suspensions, proteins can be released either after leakage or membrane shedding, which can lead to altered bioactivity of EVs [26]. Bioactivity of manufactured cryopreserved EV products will need to be checked on the long term and the HOCl-induced SSc model is a reliable model in this therapeutic indication.

Several miRNAs whose expression is altered in SSc have been proposed to be implicated in the regulation of fibrotic genes [20]. Of those, the expression of let-7a and miR-29a was shown to be down-regulated in fibroblasts or skin of SSc patients while miR-146a downregulation was detected in the peripheral blood mononuclear cells of patients [13,27,

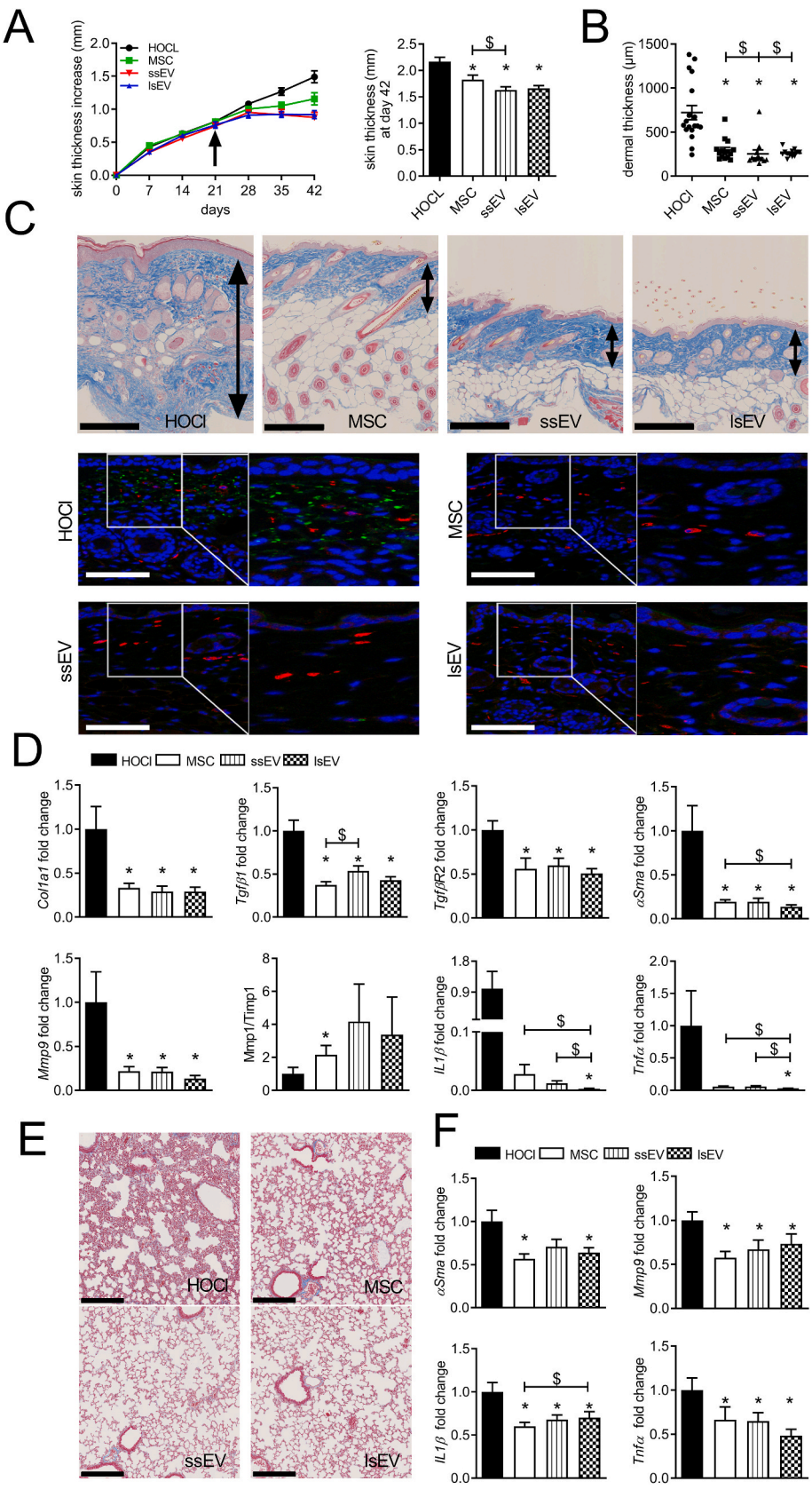

Fig. 2. Therapeutic effect of MSC-EVs in the murine model of HOCl-induced SSc. (A) Skin thickness increase in control mice (HOCl) and mice that have been injected with MSCs, small size or large size EVs (ssEVs or lsEVs, respectively) on day 21 (arrow). Mean skin thickness in the different groups of mice at day 42 (right panel). (B) Mean dermal thickness on histological sections from the different groups of mice. (C) Representative histological sections of skin after Masson's trichrome staining (double arrow delineates the dermis; scale bar, 250 µm; upper panels) and after immunostaining with antibodies specific for Tgfβ1 (green), αSma (red) and DAPI (blue) in skin (scale bar, 100 µm; enlargement x2; lower panels). (D) Gene expression in skin as expressed as fold change. (E) Representative histological sections of lungs after Masson's trichrome staining (scale bar, 250 µm). (F) Gene expression in lung samples as expressed as fold change (n = 13 to 18 per group from 2 separate experiments; *: $p < 0.05$ versus control or $: $p < 0.05$ versus the indicated group of mice). (For interpretation of the references to colour in this figure legend, the reader is referred to the Web version of this article.)

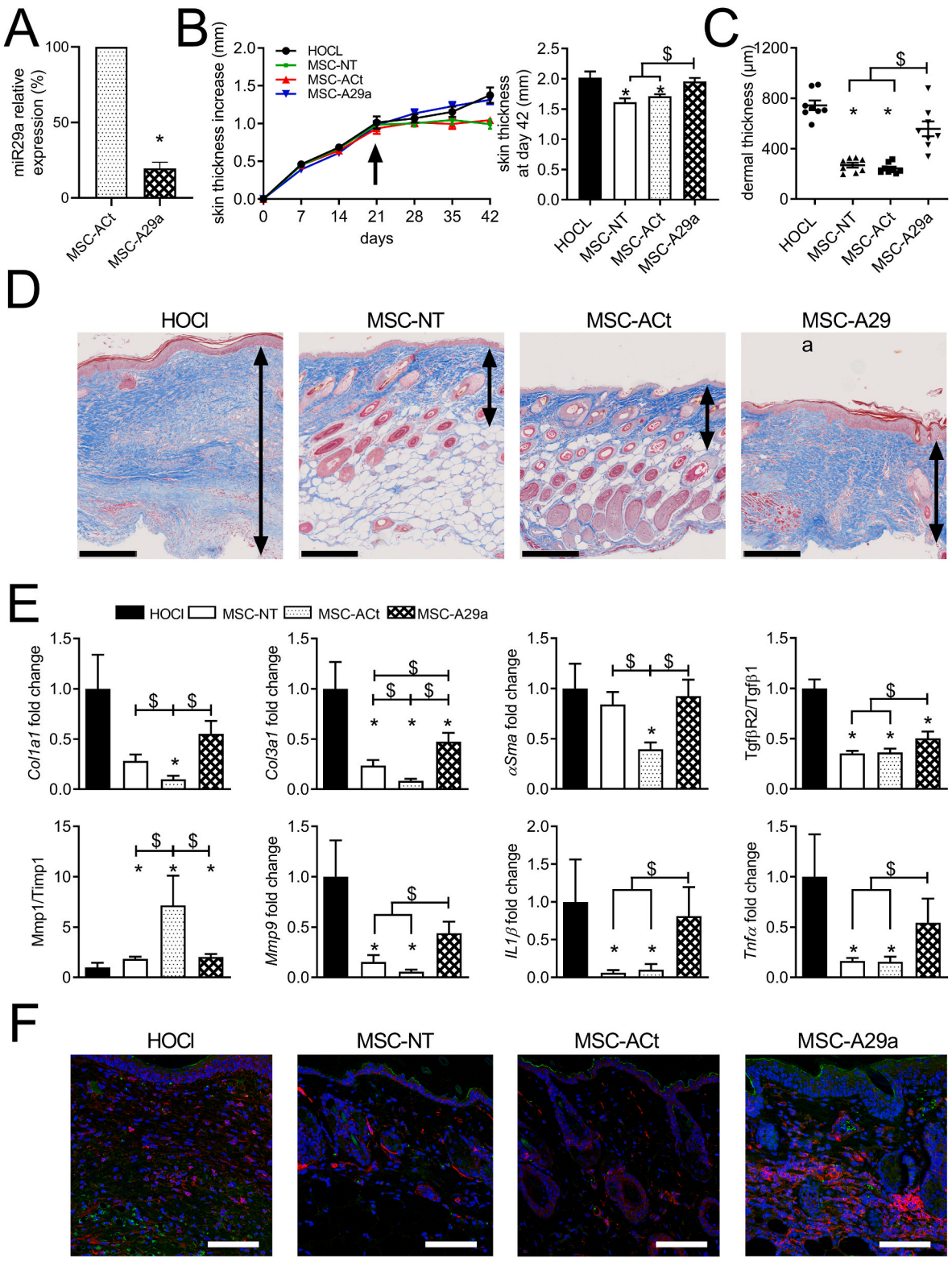

Fig. 3. Loss of the therapeutic effect of MSCs expressing low amounts of miR-29a-3p in the murine model of HOCl-induced SSc. (A) Expression of miR-29a-3p in MSCs transfected with 50 nM of antagomiR-control (MSC-ACt) or antagomiR-29a-3p (MSC-A29a). (B) Skin thickness increase in control mice (HOCl) and mice that have been injected with non-transfected MSCs (MSC-NT), MSC-ACt or MSC-A29a on day 21 (arrow). Mean skin thickness in the different groups of mice at day 42 (right panel). (C) Mean dermal thickness on histological sections of skin from the different groups of mice. (D) Representative histological sections of skin after Masson's trichrome staining (the double arrow delineates the dermis; scale bar, 250 µm). (E) Gene expression in skin samples as expressed as fold change in treated versus HOCl control mice. (F) Immunostaining with antibodies specific for Tgfβ1 (green), αSma (red) and DAPI (blue) in representative skin samples (scale bar, 100 µm). (n = 8 per group; *: $p < 0.05$ versus control or $: $p < 0.05$ versus the indicated group of mice). (For interpretation of the references to colour in this figure legend, the reader is referred to the Web version of this article.)

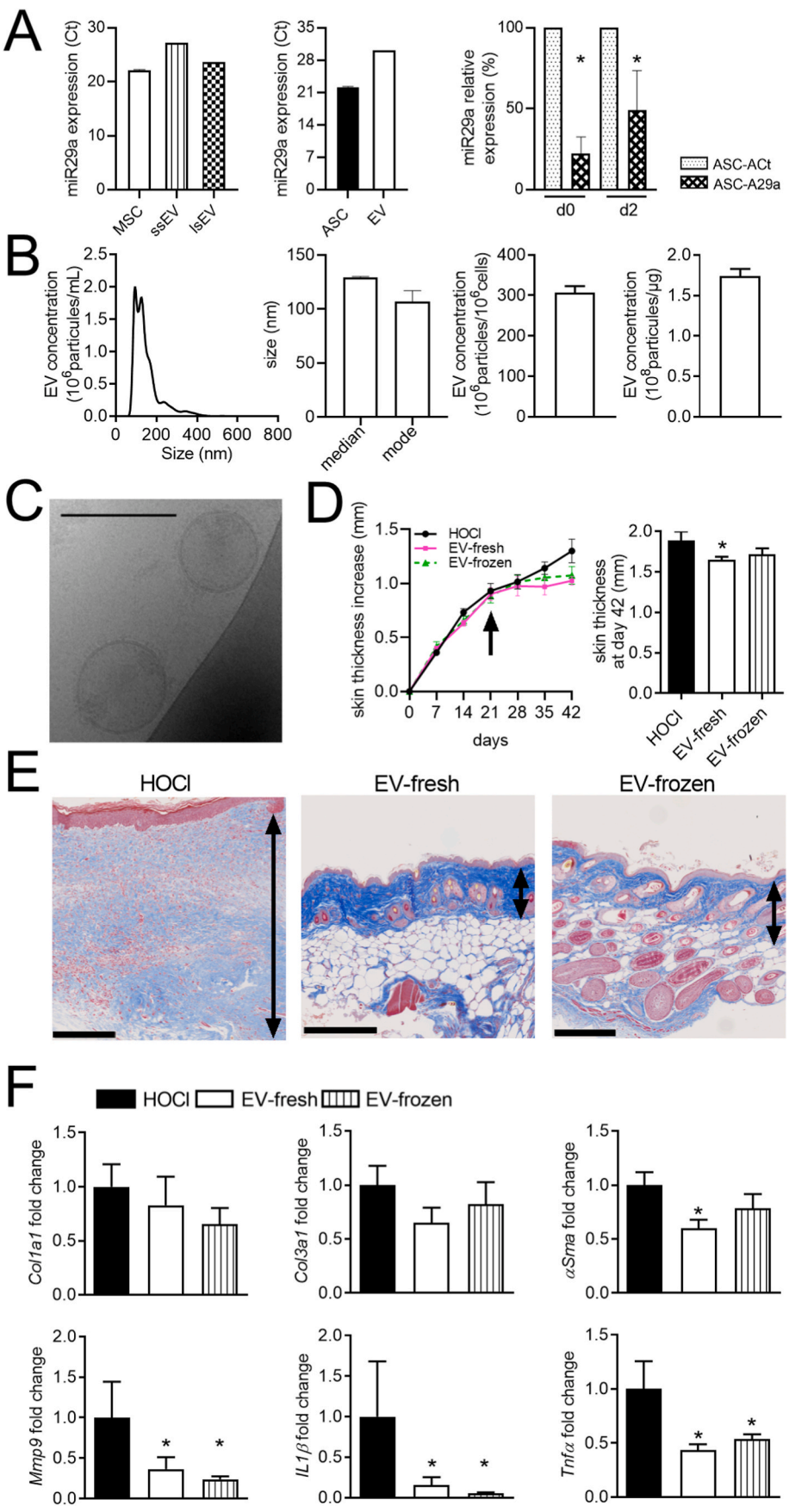

Fig. 4. Therapeutic efficiency of fresh or frozen human ASC-EVs in HOCl-induced SSc. (A) Expression of miR-29a-3p in murine MSCs (MSC), ssEVs and lsEVs, as Ct (cycle threshold) in 100 ng RNA (left panel). Expression of miR-29a-3p in human ASCs (ASC) and derived EVs (middle panel) and in ASCs transfected with antagomiR-control (ASC-ACt) or antagomiR-29a-3p (ASC-A29a) (right panel) (n = 3). (B) Size distribution and mode-median sizes of EVs assessed by NanoTracking Analysis (left panels). EV concentration is expressed as particle numbers produced by 10^6 ASCs or per µg of total proteins (n = 3). (C) Cryo-transmission electron microscopy photograph of EVs (scale bar, 200 µm). (D) Skin thickness increase in control mice (HOCl) and mice that received 4×10^7 particles of freshly prepared EVs (EV-fresh) or frozen EVs (EV-frozen) on day 21. Mean skin thickness in the different groups of mice at day 42 (right panel) (E) Representative histological sections of skin after Masson's trichrome staining (the double arrow delineates the dermis; scale bar, 250 µm). (F) Gene expression in skin samples as expressed as fold change. (n = 7–8 per group; *: $p < 0.05$ versus control).

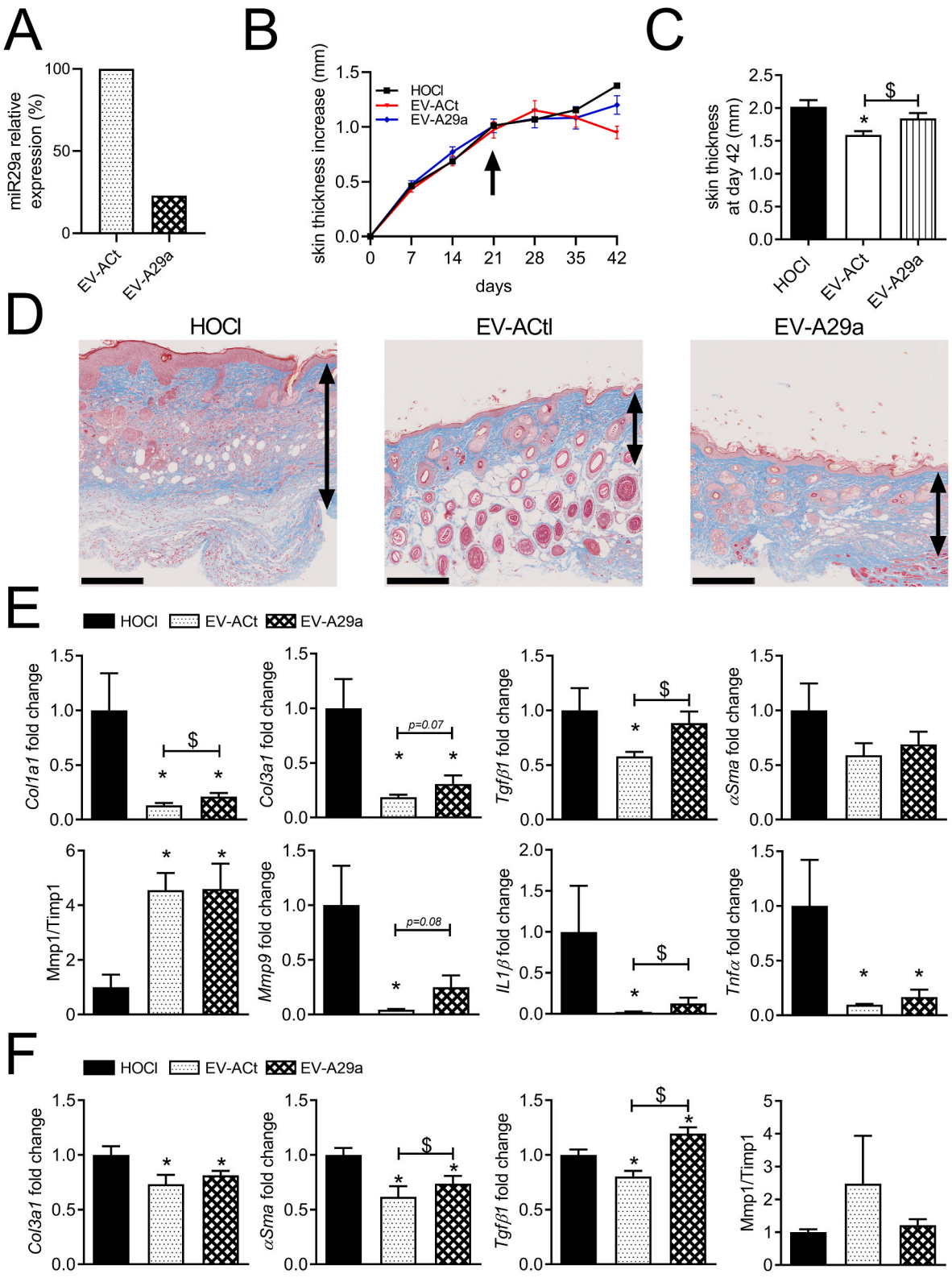

Fig. 5. Loss of the therapeutic effect of MSC-EVs expressing low amounts of miR-29a-3p in the murine model of HOCl-induced SSc. (A) Expression of miR-29a-3p in EVs from MSCs transfected with 50 nM of antagomiR-control (EV-ACt) or antagomiR-29a-3p (EV-A29a). (B) Skin thickness increase in control mice (HOCl) and mice that have been injected with EV-ACt or EV-A29a on day 21 (arrow). (C) Mean dermal thickness on histological sections of skin from the different groups of mice. (D) Representative histological sections of skin after Masson's trichrome staining (the double arrow delineates the dermis; scale bar, 250 μm). (E) Gene expression in skin samples as expressed as fold change in treated versus HOCl control mice. (F) Gene expression in lung samples as expressed as fold change in treated versus HOCl control mice. (n = 8 per group; *: $p < 0.05$ versus control or $: $p < 0.05$ versus the indicated group of mice). (For interpretation of the references to colour in this figure legend, the reader is referred to the Web version of this article.)

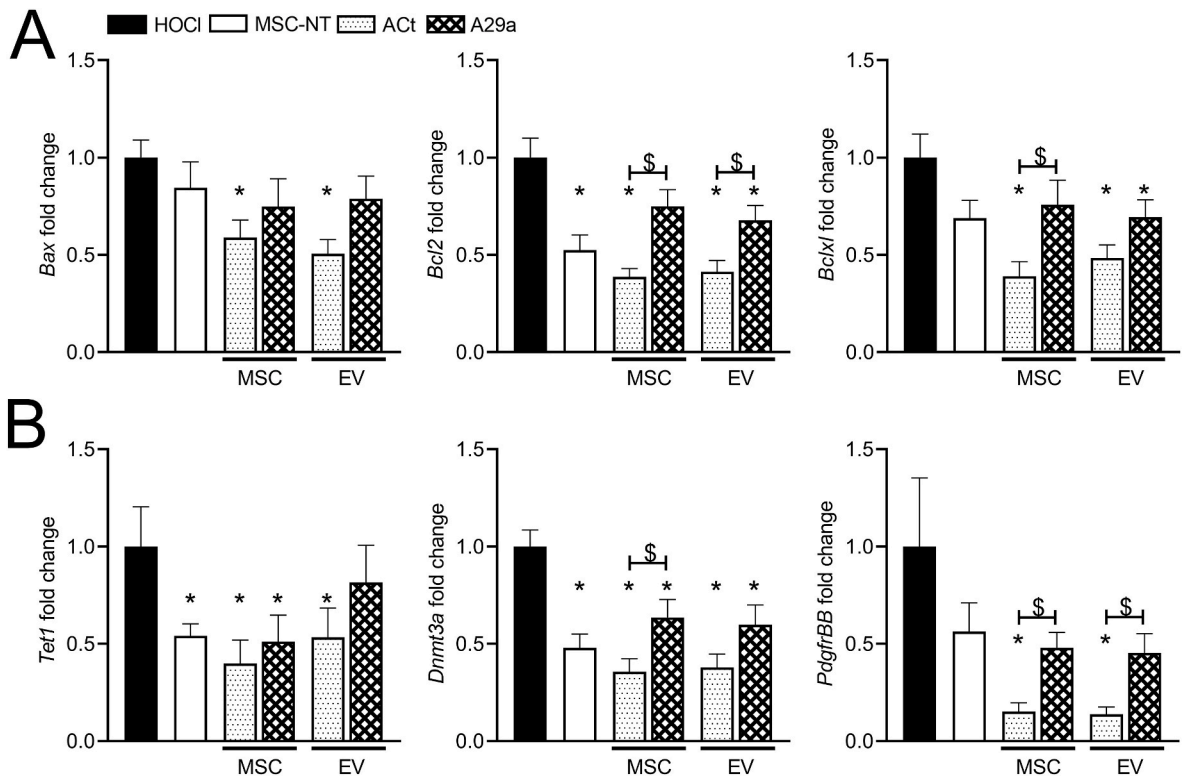

Fig. 6. Regulation of several target genes of miR-29a-3p in the skin of SSc mice. (A) Gene expression of apoptotic markers in skin samples from mice that received non-treated MSC (MSC-NT), MSC transfected with antagomiR-control (MSC-ACt) or antagomiR-29a-3p (MSC-A29a), EVs isolated from ASCs transfected with antagomiR-control (EV-ACt) or antagomiR-29a-3p (EV-A29a). (B) Gene expression of *Tet1, Dnmt3a* and *Pdgfrbb* in skin samples from same groups of mice as in A (n = 7–8 per group; *: $p < 0.05$ versus control or $: $p < 0.05$ versus the indicated group of mice).

28]. Both let-7a and miR-29a down-regulate the expression of type I and type III collagens and miR-29a was further shown to target TAB1 resulting in increased expression of MMP1 and reduced expression of TIMP1 [13,14,27]. All these factors were modulated in skin and lungs of mice treated with EVs, we therefore focused our attention on miR-29a-3p (the mature form of miR-29a). We here demonstrated its key role in the therapeutic effect of MSCs in the HOCl-induced SSc model through its release within EVs. In line with previous studies, we showed that down-regulation of miR-29a-3p in MSCs and in ASC-EVs resulted in higher levels of type I and type III collagens and a lower *Mmp1/Timp1* ratio in the skin of SSc mice. We have identified several other miRNAs in ASC-EVs, among which miR-146a (an anti-fibrotic miRNA) and miR-21, miR-155 (two pro-fibrotic miRNAs) [15,28,29]. However, the high down-regulation of miR-29a-3p in EV-A29a was associated with a slight down-regulation of these three miRNAs in ASC-EVs, independently of their role on fibrosis (data not shown). Even though we cannot exclude that other miRNAs might participate to the therapeutic function of ASC-EVs in SSc, our data suggest that miR-29a-3p is one of the major factors involved in this process.

Other targets of miR-29a-3p have been shown to be modulated in different models of fibrosis. Indeed, an inverse correlation between miR-29a-3p and MMP9 has been demonstrated in patients with lumbar spinal stenosis and MMP2 was found to be a direct target of miR-29a-3p in an experimental model of renal fibrosis [30,31]. MiR-29a is also a pro-apoptotic factor in SSc fibroblasts by disrupting the production of anti-apoptotic factors (Bcl2, BclXL) [16]. Another direct target of miR-29a-3p is Tet1, a DNA demethylase, which is deregulated in the transformation of vascular smooth muscle cells [32] and in SSc [33]. The expression of Tet1 was higher in SSc fibroblasts and increased with hypoxia, a common characteristic of SSc. Actually, global DNA hypomethylation was observed in skin suggesting an aberrant DNA methylation in the pathogenesis of SSc. Another DNA methyltransferase, Dnmt3A, is also targeted by miR-29a-3p [34]. In the fibrotic skin of SSc patients, the induction of Dnmt3A by TGFβ leads to the silencing of suppressor of cytokine signaling 3 (Socs3) by promoter hypermethylation and the downregulation of Socs3 promotes the fibroblast-to-myofibroblast transition and fibrosis [35]. Finally, miR-29a-3p was reported to target Pdgfrbb, fibrillin 1, follistatin-like 1, laminin subunit gamma 2 and other genes of the basement membrane including type 4 collagen, perlecan and osteonectin in other disease models [36–38]. Of interest, Sunitinib, an inhibitor of Pdgfrbb and vascular endothelial growth factor receptor (Vegfr) phosphorylation, reverses fibrosis in the HOCl-induced model of SSc [39]. Here, we demonstrated for the first time an inverse correlation between EV-mediated miR-29a-3p treatment and expression of *Tet1, Dnmt3a, Pdgfrbb,* in the skin of SSc mice. These data indicate that miR-29a-3p plays a critical role in regulating a variety of cellular processes and balancing numerous factors whose expression is altered in SSc.

5. Conclusion

In conclusion, the present study presents evidence that MSCs can regulate skin and lung fibrosis in SSc through the release of EVs that exert pleiotropic functions acting on different molecular pathways that are deregulated in the disease. One of the mechanisms of action displayed by MSC- and ASC-EVs is the release of miR-29a-3p that can downregulate the expression of several pro-fibrotic, remodeling and anti-apoptotic factors as well as methylases. This study highlights the role of miR-29a-3p in the murine model of HOCl-induced SSc and encourages research focusing on this miRNA and its targeted genes, especially *Dnmt3a* and *Pdgfrbb*, in the perspective of novel therapeutic options for human SSc.

Funding

We acknowledge funding support from the Inserm Institute, the University of Montpellier, the Association des Sclérodermiques de France, the Société Nationale Française de Médecine Interne, the Agence Nationale pour la Recherche for support of the national infrastructure: "ECELLFRANCE: Development of a national adult mesenchymal stem cell based therapy platform" (ANR-11-INSB-005).

Author statement

Pauline Rozier: Experimental work, data Formal analysis, manuscript writing; Marie Maumus: Experimental work, data Formal analysis; Alexandre Maria: data Formal analysis; Karine Toupet: Experimental work, data Formal analysis; Joséphine Lai-Kee-Him: Experimental work; Christian Jorgensen: Conception and design; Philippe Guilpain: Financial support, conception and design; Danièle Noel: Conception and design, data Formal analysis, manuscript writing

Data availability statement

The authors declare that all data have been provided within the manuscript.

Declaration of competing of interest

The authors declare no conflict of interest.

Acknowledgments

We thank the French National Research Agency for supporting the French Infrastructure for Integrated Structural Biology (ANR-10-INBS-05) and the national infrastructure "ECELLFRANCE: Development of a national adult mesenchymal stem cell based therapy platform" (ANR-11-INSB-005). We also acknowledge the Réseau d'Histologie Expérimentale de Montpellier" histology facility for processing our tissues and, the "SMARTY platform and Network of Animal facilities of Montpellier".

References

[1] C.P. Denton, D. Khanna, Systemic sclerosis, Lancet 390 (2017) 1685–1699, 10103.
[2] E. Zanatta, V. Codullo, J. Avouac, Y. Allanore, Systemic sclerosis: recent insight in clinical management, Joint Bone Spine, 2019.
[3] A. Tyndall, Hematopoietic stem cell transplantation for systemic sclerosis: review of current status, BioDrugs 33 (4) (2019) 401–409.
[4] A.T. Maria, K. Toupet, M. Maumus, G. Fonteneau, A. Le Quellec, C. Jorgensen, P. Guilpain, D. Noel, Human adipose mesenchymal stem cells as potent anti-fibrosis therapy for systemic sclerosis, J. Autoimmun. 70 (2016) 31–39.
[5] P. Rozier, A. Maria, R. Goulabchand, C. Jorgensen, P. Guilpain, D. Noel, Mesenchymal stem cells in systemic sclerosis: allogenic or autologous approaches for therapeutic use? Front. Immunol. 9 (2018) 2938.
[6] G. van Niel, G. D'Angelo, G. Raposo, Shedding light on the cell biology of extracellular vesicles, Nat. Rev. Mol. Cell Biol. 19 (4) (2018) 213–228.
[7] C. Thery, K.W. Witwer, E. Aikawa, M.J. Alcaraz, J.D. Anderson, R. Andriantsitohaina, A. Antoniou, T. Arab, F. Archer, G.K. Atkin-Smith, D.C. Ayre, J.M. Bach, D. Bachurski, H. Baharvand, L. Balaj, S. Baldacchino, N.N. Bauer, A. A. Baxter, M. Bebawy, C. Beckham, A. Bedina Zavec, A. Benmoussa, A.C. Berardi, P. Bergese, E. Bielska, C. Blenkiron, S. Bobis-Wozowicz, E. Boilard, W. Boireau, A. Bongiovanni, F.E. Borras, S. Bosch, C.M. Boulanger, X. Breakefield, A.M. Breglio, M.A. Brennan, D.R. Brigstock, A. Brisson, M.L. Broekman, J.F. Bromberg, P. Bryl-Gorecka, S. Buch, A.H. Buck, D. Burger, S. Busatto, D. Buschmann, B. Bussolati, E. I. Buzas, J.B. Byrd, G. Camussi, D.R. Carter, S. Caruso, L.W. Chamley, Y.T. Chang, C. Chen, S. Chen, L. Cheng, A.R. Chin, A. Clayton, S.P. Clerici, A. Cocks, E. Cocucci, R.J. Coffey, A. Cordeiro-da-Silva, Y. Couch, F.A. Coumans, B. Coyle, R. Crescitelli, M.F. Criado, C. D'Souza-Schorey, S. Das, A. Datta Chaudhuri, P. de Candia, E.F. De Santana, O. De Wever, H.A. Del Portillo, T. Demaret, S. Deville, A. Devitt, B. Dhondt, D. Di Vizio, L.C. Dieterich, V. Dolo, A.P. Dominguez Rubio, M. Dominici, M.R. Dourado, T.A. Driedonks, F.V. Duarte, H.M. Duncan, R. M. Eichenberger, K. Ekstrom, S. El Andaloussi, C. Elie-Caille, U. Erdbrugger, J. M. Falcon-Perez, F. Fatima, J.E. Fish, M. Flores-Bellver, A. Forsonits, A. Frelet-Barrand, F. Fricke, G. Fuhrmann, S. Gabrielsson, A. Gamez-Valero, C. Gardiner, K. Gartner, R. Gaudin, Y.S. Gho, B. Giebel, C. Gilbert, M. Gimona, I. Giusti, D. C. Goberdhan, A. Gorgens, S.M. Gorski, D.W. Greening, J.C. Gross, A. Gualerzi, G. N. Gupta, D. Gustafson, A. Handberg, R.A. Haraszti, P. Harrison, H. Hegyesi, A. Hendrix, A.F. Hill, F.H. Hochberg, K.F. Hoffmann, B. Holder, H. Holthofer, B. Hosseinkhani, G. Hu, Y. Huang, V. Huber, S. Hunt, A.G. Ibrahim, T. Ikezu, J. M. Inal, M. Isin, A. Ivanova, H.K. Jackson, S. Jacobsen, S.M. Jay, M. Jayachandran, G. Jenster, L. Jiang, S.M. Johnson, J.C. Jones, A. Jong, T. Jovanovic-Talisman, S. Jung, R. Kalluri, S.I. Kano, S. Kaur, Y. Kawamura, E.T. Keller, D. Khamari, E. Khomyakova, A. Khvorova, P. Kierulf, K.P. Kim, T. Kislinger, M. Klingeborn, D. J. Klinke 2nd, M. Kornek, M.M. Kosanovic, A.F. Kovacs, E.M. Kramer-Albers, S. Krasemann, M. Krause, I.V. Kurochkin, G.D. Kusuma, S. Kuypers, S. Laitinen, S. M. Langevin, L.R. Languino, J. Lannigan, C. Lasser, L.C. Laurent, G. Lavieu, E. Lazaro-Ibanez, S. Le Lay, M.S. Lee, Y.X.F. Lee, D.S. Lemos, M. Lenassi, A. Leszczynska, I.T. Li, K. Liao, S.F. Libregts, E. Ligeti, R. Lim, S.K. Lim, A. Line, K. Linnemannstons, A. Llorente, C.A. Lombard, M.J. Lorenowicz, A.M. Lorincz, J. Lotvall, J. Lovett, M.C. Lowry, X. Loyer, Q. Lu, B. Lukomska, T.R. Lunavat, S. L. Maas, H. Malhi, A. Marcilla, J. Mariani, J. Mariscal, E.S. Martens-Uzunova, L. Martin-Jaular, M.C. Martinez, V.R. Martins, M. Mathieu, S. Mathivanan, M. Maugeri, L.K. McGinnis, M.J. McVey, D.G. Meckes Jr., K.L. Meehan, I. Mertens, V.R. Minciacchi, A. Moller, M. Moller Jorgensen, A. Morales-Kastresana, J. Morhayim, F. Mullier, M. Muraca, L. Musante, V. Mussack, D.C. Muth, K. H. Myburgh, T. Najrana, M. Nawaz, I. Nazarenko, P. Nejsum, C. Neri, T. Neri, R. Nieuwland, L. Nimrichter, J.P. Nolan, E.N. Nolte-'t Hoen, N. Noren Hooten, L. O'Driscoll, T. O'Grady, A. O'Loghlen, T. Ochiya, M. Olivier, A. Ortiz, L.A. Ortiz, X. Osteikoetxea, O. Ostergaard, M. Ostrowski, J. Park, D.M. Pegtel, H. Peinado, F. Perut, M.W. Pfaffl, D.G. Phinney, B.C. Pieters, R.C. Pink, D.S. Pisetsky, E. Pogge von Strandmann, I. Polakovicova, I.K. Poon, B.H. Powell, I. Prada, L. Pulliam, P. Quesenberry, A. Radeghieri, R.L. Raffai, S. Raimondo, J. Rak, M.I. Ramirez, G. Raposo, M.S. Rayyan, N. Regev-Rudzki, F.L. Ricklefs, P.D. Robbins, D. D. Roberts, S.C. Rodrigues, E. Rohde, S. Rome, K.M. Rouschop, A. Rughetti, A. E. Russell, P. Saa, S. Sahoo, E. Salas-Huenuleo, C. Sanchez, J.A. Saugstad, M.J. Saul, R.M. Schiffelers, R. Schneider, T.H. Schoyen, A. Scott, E. Shahaj, S. Sharma, O. Shatnyeva, F. Shekari, G.V. Shelke, A.K. Shetty, K. Shiba, P.R. Siljander, A. M. Silva, A. Skowronek, O.L. Snyder 2nd, R.P. Soares, B.W. Sodar, C. Soekmadji, J. Sotillo, P.D. Stahl, W. Stoorvogel, S.L. Stott, E.F. Strasser, S. Swift, H. Tahara, M. Tewari, K. Timms, S. Tiwari, R. Tixeira, M. Tkach, W.S. Toh, R. Tomasini, A. C. Torrecilhas, J.P. Tosar, V. Toxavidis, L. Urbanelli, P. Vader, B.W. van Balkom, S. G. van der Grein, J. Van Deun, M.J. van Herwijnen, K. Van Keuren-Jensen, G. van Niel, M.E. van Royen, A.J. van Wijnen, M.H. Vasconcelos, I.J. Vechetti Jr., T. D. Veit, L.J. Vella, E. Velot, F.J. Verweij, B. Vestad, J.L. Vinas, T. Visnovitz, K. V. Vukman, J. Wahlgren, D.C. Watson, M.H. Wauben, A. Weaver, J.P. Webber, V. Weber, A.M. Wehman, D.J. Weiss, J.A. Welsh, S. Wendt, A.M. Wheelock, Z. Wiener, L. Witte, J. Wolfram, A. Xagorari, P. Xander, J. Xu, X. Yan, M. Yanez-Mo, H. Yin, Y. Yuana, V. Zappulli, J. Zarubova, V. Zekas, J.Y. Zhang, Z. Zhao, L. Zheng, A.R. Zheutlin, A.M. Zickler, P. Zimmermann, A.M. Zivkovic, D. Zocco, E. K. Zuba-Surma, Minimal information for studies of extracellular vesicles 2018 (MISEV2018): a position statement of the International Society for Extracellular Vesicles and update of the MISEV2014 guidelines, J. Extracell. Vesicles 7 (1) (2018), 1535750.
[8] S. Cosenza, M. Ruiz, M. Maumus, C. Jorgensen, D. Noel, Pathogenic or therapeutic extracellular vesicles in rheumatic diseases: role of mesenchymal stem cell-derived vesicles, Int. J. Mol. Sci. 18 (4) (2017).
[9] J.S. Rockel, R. Rabani, S. Viswanathan, Anti-fibrotic mechanisms of exogenously-expanded mesenchymal stromal cells for fibrotic diseases, Semin. Cell Dev. Biol. 101 (2020) 87–103.
[10] Y. Kawashita, M. Jinnin, T. Makino, I. Kajihara, K. Makino, N. Honda, S. Masuguchi, S. Fukushima, Y. Inoue, H. Ihn, Circulating miR-29a levels in patients with scleroderma spectrum disorder, J. Dermatol. Sci. 61 (1) (2011) 67–69.
[11] R. Takemoto, M. Jinnin, Z. Wang, H. Kudo, K. Inoue, W. Nakayama, A. Ichihara, T. Igata, I. Kajihara, S. Fukushima, H. Ihn, Hair miR-29a levels are decreased in patients with scleroderma, Exp. Dermatol. 22 (12) (2013) 832–833.
[12] L. Zhang, H. Wu, M. Zhao, Q. Lu, Meta-analysis of differentially expressed microRNAs in systemic sclerosis, Int. J. Rheum. Dis 23 (10) (2020) 1297–1304.
[13] B. Maurer, J. Stanczyk, A. Jungel, A. Akhmetshina, M. Trenkmann, M. Brock, O. Kowal-Bielecka, R.E. Gay, B.A. Michel, J.H. Distler, S. Gay, O. Distler, MicroRNA-29, a key regulator of collagen expression in systemic sclerosis, Arthritis Rheum. 62 (6) (2010) 1733–1743.
[14] M. Ciechomska, S. O'Reilly, M. Suwara, K. Bogunia-Kubik, J.M. van Laar, MiR-29a reduces TIMP-1 production by dermal fibroblasts via targeting TGF-beta activated kinase 1 binding protein 1, implications for systemic sclerosis, PloS One 9 (12) (2014), e115596.
[15] S. Jafarinejad-Farsangi, F. Gharibdoost, A. Farazmand, H. Kavosi, A. Jamshidi, E. Karimizadeh, F. Noorbakhsh, M. Mahmoudi, MicroRNA-21 and microRNA-29a modulate the expression of collagen in dermal fibroblasts of patients with systemic sclerosis, Autoimmunity 52 (3) (2019) 108–116.
[16] S. Jafarinejad-Farsangi, A. Farazmand, M. Mahmoudi, F. Gharibdoost, E. Karimizadeh, F. Noorbakhsh, H. Faridani, A.R. Jamshidi, MicroRNA-29a induces apoptosis via increasing the Bax:Bcl-2 ratio in dermal fibroblasts of patients with systemic sclerosis, Autoimmunity 48 (6) (2015) 369–378.
[17] C. Bouffi, C. Bony, G. Courties, C. Jorgensen, D. Noel, IL-6-dependent PGE2 secretion by mesenchymal stem cells inhibits local inflammation in experimental arthritis, PloS One 5 (12) (2010), e14247.
[18] M. Maumus, C. Manferdini, K. Toupet, J.A. Peyrafitte, R. Ferreira, A. Facchini, E. Gabusi, P. Bourin, C. Jorgensen, G. Lisignoli, D. Noel, Adipose mesenchymal stem cells protect chondrocytes from degeneration associated with osteoarthritis, Stem Cell Res. 11 (2) (2013) 834–844.
[19] H. Jiang, G. Zhang, J.H. Wu, C.P. Jiang, Diverse roles of miR-29 in cancer (review), Oncol. Rep. 31 (4) (2014) 1509–1516.

[20] M. Colletti, A. Galardi, M. De Santis, G.M. Guidelli, A. Di Giannatale, L. Di Luigi, C. Antinozzi, Exosomes in systemic sclerosis: messengers between immune, vascular and fibrotic components? Int. J. Mol. Sci. 20 (18) (2019).
[21] S. Guiducci, J.H. Distler, A. Jungel, D. Huscher, L.C. Huber, B.A. Michel, R.E. Gay, D.S. Pisetsky, S. Gay, M. Matucci-Cerinic, O. Distler, The relationship between plasma microparticles and disease manifestations in patients with systemic sclerosis, Arthritis Rheum. 58 (9) (2008) 2845–2853.
[22] P.J. Wermuth, S. Piera-Velazquez, S.A. Jimenez, Exosomes isolated from serum of systemic sclerosis patients display alterations in their content of profibrotic and antifibrotic microRNA and induce a profibrotic phenotype in cultured normal dermal fibroblasts, Clin. Exp. Rheumatol. 35 (2017) 21–30. Suppl 106(4).
[23] C. Chen, D. Wang, A. Moshaverinia, D. Liu, X. Kou, W. Yu, R. Yang, L. Sun, S. Shi, Mesenchymal stem cell transplantation in tight-skin mice identifies miR-151-5p as a therapeutic target for systemic sclerosis, Cell Res. 27 (4) (2017) 559–577.
[24] S. Cosenza, K. Toupet, M. Maumus, P. Luz-Crawford, O. Blanc-Brude, C. Jorgensen, D. Noel, Mesenchymal stem cells-derived exosomes are more immunosuppressive than microparticles in inflammatory arthritis, Theranostics 8 (5) (2018) 1399–1410.
[25] A. Jeyaram, S.M. Jay, Preservation and storage stability of extracellular vesicles for therapeutic applications, AAPS J. 20 (1) (2017) 1.
[26] R. Maroto, Y. Zhao, M. Jamaluddin, V.L. Popov, H. Wang, M. Kalubowilage, Y. Zhang, J. Luisi, H. Sun, C.T. Culbertson, S.H. Bossmann, M. Motamedi, A. R. Brasier, Effects of storage temperature on airway exosome integrity for diagnostic and functional analyses, J. Extracell. Vesicles 6 (1) (2017) 1359478.
[27] K. Makino, M. Jinnin, A. Hirano, K. Yamane, M. Eto, T. Kusano, N. Honda, I. Kajihara, T. Makino, K. Sakai, S. Masuguchi, S. Fukushima, H. Ihn, The downregulation of microRNA let-7a contributes to the excessive expression of type I collagen in systemic and localized scleroderma, J. Immunol. 190 (8) (2013) 3905–3915.
[28] M. Vreca, M. Andjelkovic, N. Tosic, A. Zekovic, N. Damjanov, S. Pavlovic, V. Spasovski, Impact of alterations in X-linked IRAK1gene and miR-146a on susceptibility and clinical manifestations in patients with systemic sclerosis, Immunol. Lett. 204 (2018) 1–8.
[29] C.M. Artlett, S. Sassi-Gaha, J.L. Hope, C.A. Feghali-Bostwick, P.D. Katsikis, Mir-155 is overexpressed in systemic sclerosis fibroblasts and is required for NLRP3 inflammasome-mediated collagen synthesis during fibrosis, Arthritis Res. Ther. 19 (1) (2017) 144.
[30] G. Castoldi, C. di Gioia, F. Giollo, R. Carletti, C. Bombardi, M. Antoniotti, F. Roma, G. Zerbini, A. Stella, Different regulation of miR-29a-3p in glomeruli and tubules in an experimental model of angiotensin II-dependent hypertension: potential role in renal fibrosis, Clin. Exp. Pharmacol. Physiol. 43 (3) (2016) 335–342.
[31] G. Zhang, W. Zhang, Y. Hou, Y. Chen, J. Song, L. Ding, Detection of miR29a in plasma of patients with lumbar spinal stenosis and the clinical significance, Mol. Med. Rep. 18 (1) (2018) 223–229.
[32] Z.L. Jiang, J.T. Liu, Z. Liu, Y. Chen, Y. Qi, Q. Yao, Microrna-29a involvement in phenotypic transformation of venous smooth muscle cells via Tet1 in response to mechanical cyclic stretch, J. Biomech. Eng. (2019).
[33] M. Hattori, Y. Yokoyama, T. Hattori, S. Motegi, H. Amano, I. Hatada, O. Ishikawa, Global DNA hypomethylation and hypoxia-induced expression of the ten eleven translocation (TET) family, TET1, in scleroderma fibroblasts, Exp. Dermatol. 24 (11) (2015) 841–846.
[34] G. Song, L. Tian, Y. Cheng, J. Liu, K. Wang, S. Li, T. Li, Antitumor activity of sevoflurane in HCC cell line is mediated by miR-29a-induced suppression of Dnmt3a, J. Cell. Biochem. 120 (10) (2019) 18152–18161.
[35] C. Dees, S. Potter, Y. Zhang, C. Bergmann, X. Zhou, M. Luber, T. Wohlfahrt, E. Karouzakis, A. Ramming, K. Gelse, A. Yoshimura, R. Jaenisch, O. Distler, G. Schett, J.H. Distler, TGF-beta-induced epigenetic deregulation of SOCS3 facilitates STAT3 signaling to promote fibrosis, J. Clin. Invest. 130 (5) (2020) 2347–2363.
[36] A. Galimov, T.L. Merry, E. Luca, E.J. Rushing, A. Mizbani, K. Turcekova, A. Hartung, C.M. Croce, M. Ristow, J. Krutzfeldt, MicroRNA-29a in adult muscle stem cells controls skeletal muscle regeneration during injury and exercise downstream of fibroblast growth factor-2, Stem Cell. 34 (3) (2016) 768–780.
[37] R. Ma, M. Wang, S. Gao, L. Zhu, L. Yu, D. Hu, L. Zhu, W. Huang, W. Zhang, J. Deng, J. Pan, H. He, Z. Gao, J. Xu, X. Han, miR-29a promotes the neurite outgrowth of rat neural stem cells by targeting extracellular matrix to repair brain injury, Stem Cell. Dev. 29 (9) (2020) 599–614.
[38] K. Wang, J. Yu, B. Wang, H. Wang, Z. Shi, G. Li, miR-29a regulates the proliferation and migration of human arterial smooth muscle cells in arteriosclerosis obliterans of the lower extremities, Kidney Blood Press. Res. 44 (5) (2019) 1219–1232.
[39] N. Kavian, A. Servettaz, W. Marut, C. Nicco, C. Chereau, B. Weill, F. Batteux, Sunitinib inhibits the phosphorylation of platelet-derived growth factor receptor beta in the skin of mice with scleroderma-like features and prevents the development of the disease, Arthritis Rheum. 64 (6) (2012) 1990–2000.